Isomerism of the Aniline Trimer**

Cristóbal Pérez, Iker León, Alberto Lesarri,* Brooks H. Pate, Rodrigo Martínez,

Judith Millán, José A. Fernández

[*]   Dr. C. Pérez,

Deutsches Elektronen-Synchrotron DESY, Notkestrasse 85, D-22607 Hamburg (Germany); Departamento de Química Física, Universidad del País Vasco, 48940 Leioa (Spain); Ikerbasque, Basque Foundation for Science, 48013 Bilbao (Spain)

Dr. I. León, Prof. A. Lesarri

Departamento de Química Física y Química Inorgánica, Universidad de Valladolid, 47011 Valladolid (Spain) E-mail: lesarri@qf.uva.es, Web: www.uva.es/lesarri

Prof. B. H. Pate

Department of Chemistry, University of Virginia, McCormick Rd., Charlottesville, VA 22904 (USA)

Dr. R. Martínez, Dr. J. Millán

Departamento de Química, Universidad de La Rioja, 26006 Logroño (Spain)

Dr. J. A. Fernández

Departamento de Química Física, Universidad del País Vasco, 48080 Bilbao (Spain)

Abstract

Weaker intermolecular forces expand the isomerization alternatives for molecular aggregation, as observed for the prototype models of the aniline trimer (An_3) and the monohydrated aniline dimer (An_2-W) when compared to the phenol trimer. In this experiment the aniline clusters were generated in a jet-cooled expansion and probed using broadband (chirped-pulsed) microwave spectroscopy. Three isomers of the aniline trimer and two isomers of the hydrated dimer were detected and characterized in the rotational spectrum. In the homotrimer the weak N-H···N hydrogen bonds are assisted by subtle combinations of N-H···π and C-H···π interactions, producing several competing low-lying ring species in the gas phase. One of the aniline trimers is a symmetric top, topologically equivalent to the only observed phenol trimer. Conversely, addition of a water molecule to the aniline dimer introduces a leading O-H···N interaction, making water to behave as dominant hydrogen-bond pivot between the two aniline molecules. This combination of weak intermolecular interactions critically tests the performance of dispersion-corrected or parametrized density-functional methods. Evaluation of the B3LYP-D3(BJ) and M06-2X methods revealed deficiencies of the Truhlar functional to reproduce the experimental rotational data.

The portfolio of non-covalent interactions has expanded from conventional hydrogen bonds to a large number of chemical groups and diverse intermolecular forces of variable strength (2-60 kJ mol^{-1}).[1] Examples include the attraction of σ-hole electrophilic regions in halogen, chalcogen, pnictogen or tetrel bonds[2] or the weak hydrogen bonds to π acceptors, radicals and metal centers.[1,3] The disparity of molecular forces results in specific structural issues such as delicate conformational equilibria, binding competition or cooperativity.[4] In consequence, there is a demand for experimental data on isolated (interaction-specific) intermolecular clusters and computational models accounting for the weaker non-covalent forces, in particular dispersion.

Neutral molecular clusters can be generated in supersonic jet expansions and characterized with high-resolution spectroscopy. Vibronic laser techniques reveal conformational composition and supramolecular aggregation,[5,6] but structural information is gained indirectly through the vibrational modes.[7,8,9] Rotational spectroscopy provides atomic resolution, but its application to trimers or larger aggregates is limited to a few examples.[10,11,12] The aniline trimers are challenging prototype models for non-covalent bonding in amines, weaker and less studied than those involving other functional groups, in particular alcohols. Moreover, the weak donor/acceptor character of the amino group and the aromatic ring offer binding competition through a vast array of N-H⋯N,[13] N-H⋯π,[14] C-H⋯π[15] and π⋯π[16] interactions, plus the O-H⋯N[17] and N-H⋯O[18] hydrogen bonds in the hydrate. The aniline trimer offers direct comparison with the phenol homomers, where the much stronger O-H⋯O hydrogen bond produces a single isomer for the dimer and trimer in the gas phase.[7,10] No other trimers of similar size have been reported with rotational resolution. Finally, large intermolecular clusters are extremely floppy systems hard to model with molecular orbital methods,[19,20] as evidenced by the development of specific databases (GMTKN30,[21] BEGDB,[22] NCI[23],

S12L[24]) and dispersion-corrected density-functional theory (DFT).[25,26] In the aniline trimers computing difficulties are expected to grow as weaker interactions become dominant. Presently, no structural benchmarks exist comparing rotational data for the aniline trimers or similarly sized clusters and ab initio or DFT calculations.

We report here comprehensive rotational data on the aniline homotrimer and the monohydrated aniline dimer. We will show how the weak interactions in the trimers result in unique multiple isomerism and conformational equilibria for the two clusters. The experimental results will produce rotational benchmarking information concerning two representative DFT computational strategies and previous spin-component-scaled local MP2 (SCS-LMP2) calculations by Schütz.[27] Predictions using both a parametrized functional (M06-2X[25]) and dispersion-corrected DFT energies (B3LYP-D3(BJ)[26]) will be evaluated. The results will illustrate the balance of forces in the aniline trimers, simultaneously revealing shortcomings of the DFT models. Finally, analysis of the reduced electron density will help describing the physical forces in the clusters. Our model selection was justified by a previous analysis of vibrational data using M06-2X[28] and the documented performance of D3 corrections in rotational[29] and vibrational[30] experiments.

The experiment probed a jet expansion of aniline, using neon as carrier gas. The rotational spectrum was measured in the region 2-8 GHz with broadband fast-passage microwave spectroscopy,[31] using different configurations (see SI). The final spectrum was recorded at the University of Virginia.[12] In these experiments a microwave chirped-pulse excites the polar molecules, recording the full-band spectrum in a single event. The initial records of aniline immediately detected the monomer,[32] the monohydrated dimer[33] and the neon cluster,[34] the dimer being symmetry-inactive.[35] The vibrational ground-state of aniline is split in two nitrogen-inversion sublevels, but only the lowest-

lying state was populated under jet-cooled conditions. Further search for the aniline trimer proved initially unsuccessful. A positive observation was obtained using ^{15}N-aniline, where cancellation of nuclear quadrupole hyperfine effects enhances transition intensity. Two different asymmetric rotors were first identified, corresponding to independent isomers of the homotrimer (An$_3$-I and An$_3$-II). The rotational spectra in Figures 1 and S1 (SI) showed unequivocal transition patterns and opposite selection rules (An$_3$-I: $\mu_b \sim \mu_c > \mu_a \sim 0$; An$_3$-II: $\mu_a > \mu_c > \mu_b$). Finally, we discovered the characteristic pattern of an ideal symmetric rotor, evidencing a third isomer of the trimer (An$_3$-III, Figure S2, SI). Addition of water vapor to the jet generated the monohydrated aniline dimer An$_2$-W, for which two different isomers were identified (An$_2$-W-I: $\mu_b > \mu_c > \mu_a \sim 0$; An$_2$-W-II: $\mu_a > \mu_b \sim \mu_c \sim 0$, Figures 1 and S3). The assignment of the hydrates was confirmed by observation of the ^{18}O-water isotopologues. The spectrum did not reveal tunneling splittings associated to large amplitude motions, so the observed transitions were reproduced with a semirigid-rotor Hamiltonian. The experimental rotational parameters are collected in Tables 1 and S1 (transition frequencies in Tables S2-S8, SI).

The conformational assignment was assisted by computational calculations (SI). Two DFT models were tested. Initially, a molecular mechanics conformational search was refined with the M06-2X[25] functional and a Pople triple-ζ basis set (6-311++G(d,p)). The 30 lower-energy isomers (<25 kJ/mol) and four structures predicted by Schütz[27] are collected in Tables S9-S10 (SI). In a second step, all isomers were reoptimized using Grimme's D3 empirical dispersion with the Becke-Johnson D3(BJ)[26] damping function and Ahlrichs' triple-ζ basis set (def2-TZVP), which converged to 26 isomers (Tables S11-S12, SI). Reoptimization with a different computational method occasionally led to different minima, emphasizing the difficulty to model the weak interactions in the trimers.

The computational performance was evaluated in terms of the observed rotational constants and predicted structures. Noticeably, we observed that M06-2X failed to correctly reproduce the structures for both the aniline trimer and the hydrated dimer, exposing relative differences (rd) above 10% even for the lowest-lying isomers (Table S10, SI). Deficiencies of M06-2X to discriminate between O-H⋯O and O-H⋯π non-covalent interactions have been noticed before.[30] The B3LYP-D3(BJ) results offer much better agreement and a confident conformational assignment. The first isomer of the aniline trimer (An_3-I), identified as isomer 14, was coincident with the most stable isomer of Schütz[27] and exhibits relative deviations below 1.5% (Tables S12-S13, SI), remarkably good for a cluster of this size. The assignment of the third species An_3-III as isomer 5 was also obvious, as this was the only predicted symmetric rotor and the agreement with the experiment was also excellent (rd<0.8%). The assignment of the second trimer species was more difficult, as two isomers (1 and 23) would offer an acceptable match (rd=5.5-7.9% and 1.1-5.3%, respectively in Table S12), and a comparison of the observed selection rules and predicted electric dipole moments was not conclusive either. On the other hand, energetic arguments point to structure 1 as the most probable candidate. Isomer 1 is predicted among the most stable structures independently of the theoretical method. Interestingly, the detailed conformational search of Schütz[27] did not find isomers II and III, and at the same time three out of four of his predicted isomers do not apparently exist in the gas phase (Table S13, SI). This situation again illustrates the difficulties for a conformational search in shallow potential surfaces involving weak non-covalent interactions.

In the hydrated dimer An_2-W water produces stronger hydrogen bond interactions, yet again the M06-2X computations (Tables S14-S15, SI) did not provide a secure assignment. Conversely, B3LYP-D3(BJ) produced again an unequivocal match

identifying An_2-H_2O-I as isomer 1 (rd<1.1%, Tables S16-S17, SI) and An_2-H_2O-II as isomer 13 (rd<4.5%). The electronic, Gibbs (298 K) and complexation energies for all predicted isomers are collected in Tables S9-S17 (SI). B3LYP-D3(BJ) predicted the trimer An_3-I (isomer 14=S1) with the largest binding energy (ΔE_c= -78.8 kJ mol^{-1}), as in the previous SCS-LMP2 calculations (-65.5 kJ mol^{-1}).[27] Three more isomers (1, 5, 2) were predicted within 2.7 kJ mol^{-1}, of which the first two were observed. Five other isomers have complexation energies 5.6-7.0 kJ mol^{-1} larger, with the rest exceeding differences of 10 kJ mol^{-1}. For the hydrated dimer the two observed isomers (13, 1) are practically isoenergetic (ΔE_c= -74.9 and -74.4 kJ mol^{-1}), with differences with all other isomers exceeding 4.3 kJ mol^{-1}. Complexation energies are graphically illustrated in Figures S4 and S5 (SI). This energetic description is coherent with the experimental findings, but the noticeable differences between the two DFT and SCS-LMP2 calculations are indicative of model uncertainties, which showcases the difficulties of the current models to predict a definitive energy ordering.

The predicted geometries of the aniline trimers and a 3D mapping of the non-covalent interactions are shown in Figures 2-3, S6-S10 (rotatable), S11 (oxygen coordinates in the monohydrate) and Tables S18-24. The intermolecular interactions were categorized on the basis of a NCI analysis,[36] based on a reduced density gradient of the electron density. The contributions to the Laplacian of the density along the axes of maximal variation serve to characterize the intermolecular interactions as hydrogen bonds, non-bonding or dispersive interactions, producing a quantitative spatial description of the forces stabilizing the clusters.[37] The observed topology of the three aniline trimers differs considerably. An_3-I is based on a network of two consecutive N-H···N hydrogen bonds (D3(BJ): r(N-H···N)=2.16-2.17 Å), reminiscent of the cooperative networks observed for the hydroxyl group in the phenol[10] or water

trimers.[38] However, the near-antiparallel orientation of the first two aniline molecules prevents closing a ring of three amino groups, instead displaying an N-H···π bond between the third and first molecules (r(N-H···π)=2.58 Å). Conversely, An$_3$-II presents a single N-H···N contact (=2.13 Å), with the third aniline molecule involved in N-H···π interactions with the other two monomers (=2.51-2.84 Å). The symmetric top An$_3$-III is made of a network of three simultaneous N-H···N (=2.21 Å) and C-H···π hydrogen bonds. Unlike in the phenol or water trimers B3LYP-D3(BJ) does not predict significative cooperative effects that would shrink the N-H···N bond length. The N-H···N hydrogen bonds are within the range of R-NH$_2$···N(sp^2) interactions in crystals (1.83-2.30 Å).[39] The two isomers of An$_2$-W in Figure 3 are radically different by the presence of stronger O-H···N hydrogen bonds and built on modified aniline-water[33] dimers. In isomer An$_2$-W-I the three polar groups establish three chained N-H···O-H···N-H hydrogen bonds, closing a six-membered ring. The O-H···N interaction exhibits the shorter bond distance (=1.93 Å), followed by N-H···O and N-H···N (=2.13 Å and 2.21 Å, respectively). The O-H···N bond length in aniline-water is slightly larger (1.995 Å[33]) but within the 1.93-2.03 Å range observed for OH···N(sp^2) crystals.[40] In An$_2$-W-II the last N-H group is linked to the second aniline though N-H···π interactions (=2.54 Å). In both isomers the two rings are close to perpendicular arrangements, engaging through C-H···π interactions.

In conclusion, we combined rotational and computational data to establish the isomerization properties of the aniline trimer and the monohydrated aniline dimer, reporting rotational evidence for five different trimers. The aniline trimer and the monohydrated dimer differ in the stronger interactions caused by the water OH group. In the aniline trimer the weak character of the N-H···N hydrogen bond does not suffice to control the cluster geometry, as the network configuration of three successive hydrogen

bonds can be equalized by alternative configurations with one or two N-H⋯N bonds supplemented by N-H⋯ π and C-H⋯π interactions. In the monohydrated dimer the water molecule plays a pivotal role based in the stronger O-H⋯N hydrogen bond. The balance of weak non-covalent forces alternating between ring or chain structures has been observed before,[9] but the structural detail of the present rotational study is unprecedented for a cluster of this molecular size. In particular, the reduced stability of the symmetric top aniline trimer compared to phenol questions whether this kind of regular geometries will be present for even weaker interactions, calling for additional experiments with lower electronegativity atoms. The advantages of a direct comparison between rotational data and computational calculations proves valuable to assess the performance of the DFT methods.[41] As previously observed in related clusters the structural description of the B3LYP-D3(BJ) model is satisfactorily for the present spectroscopic purposes,[24,29,30] but the energetic description is unclear and the conformational search still pose considerable difficulties. In particular, it is difficult to correlate energetic properties and jet populations, which might be kinetically controlled by multi-body collisions benefiting specific structures less stable thermodynamically.[42] A full description of the jet populations would require a description of the conformational relaxation paths, a formidable task out of the scope of our experiment. The experimental results presented here will surely provide guidance on further development of empirical potentials and other computational methods to describe the subtle balance of intra and intermolecular interactions at play in molecular systems of increasing size.

REFERENCES

[1] S. Scheiner (Ed.), *Noncovalent Forces*, Springer, Heidelberg, **2015**.

[2] A. C. Legon, *Phys. Chem. Chem. Phys*., **2017**, *19*, 14884.

[3] G. R. Desiraju, T. Steiner, *The Weak Hydrogen Bond*, Oxford Univ. Press, Oxford, **1999**.

[4] A. S. Mahadevi, G. N. Sastry, *Chem. Rev*. **2016**, *116*, 2775.

[5] U. Buck, C. C. Pradzynski, T. Zeuch, J. M. Dieterich, B. Hartke, *Phys. Chem. Chem Phys.* **2014**, *16*, 6859.

[6] D. P. Tabor, R. Kusaka, P. S. Walsh, T. S. Zwier, E. L. Sibert III, *J. Phys. Chem. A* **2015**, *119*, 9917.

[7] T. Ebata, T. Watanabe, N. Mikami, *J. Phys. Chem.*, **1995**, *99*, 5761.

[8] a) I. León, J. Millán, E. J. Cocinero, A. Lesarri, J. A. Fernández, *Angew. Chem. Int. Ed.* **2014**, *53*, 12480. b) I. León, J. Millán, E. J. Cocinero, A. Lesarri, J. A. Fernández, *Phys. Chem. Chem. Phys*. **2014**, *16*, 23301.

[9] T. Forsting, H. C. Gottschalk, B. Hartwig, M. Mons, M. A. Suhm, *Phys. Chem. Chem Phys.* **2017**, *19*, 10727.

[10] N. A. Seifert, A. L. Steber, J. L. Neill, C. Pérez, D. P. Zaleski, B. H, Pate, A. Lesarri, *Phys. Chem. Chem. Phys*. **2013**, *15*, 11468.

[11] a) J. Thomas, N. A. Seifert, W. Jäger, Y. Xu, *Angew. Chem. Int. Ed.* **2017**, *56*, 6289. b) J. Thomas, X. Liu, W. Jäger, Y. Xu, *Angew. Chem. Int. Ed*. **2015**, 54, 11711. c) G. Feng, L. Evangelisti, I. Cacelli, L. Carbonaro, G. Prampolini, W. Caminati, *Chem. Comm*. **2014**, 50, 171. d) C. Calabrese, L. Evangelisti, I. Uriarte, B. H. Pate, E. J. Cocinero, Comm. B7.2, *25th Int. Conf. High Res. Mol. Spectroscopy*, Bilbao, 2018.

[12] a) C. Pérez, M. T. Muckle, D. P. Zaleski, N. A. Seifert, B. Temelso, G. C. Shields, Z. Kisiel, B. H. Pate, *Science* **2012**, *336*, 897. b) C. Pérez, S. Lobsiger, N. A. Seifert, D. P. Zaleski, B. Temelso, G. C. Shields, Z. Kisiel, B. H. Pate, *Chem. Phys. Lett.* **2013**, *571*, 1.

[13] a) J. C. Mullaney, D. P. Zaleski, D. P. Tew, N. R. Walker, A. C. Legon, *ChemPhysChem* **2016**, *17*, 1154. b) V. Bertolasi, P. Gili, V. Ferretti, G. Gilli, C. Fernández-Castaño, *Acta Cryst.* **1999**, *B55*, 985. c) A. L. Llamas-Saiz, C. Foces-Foces, *J. Mol. Struct.* **1990**, *238*, 367.

[14] a) C. Pfaffen, D. Infanger, P. Ottiger, H.-M. Frey, S. Leutwyler, *Phys. Chem. Chem. Phys*. **2011**, *13*, 14110. b) P. Ottiger, C. Pfaffen, R. Leist, S. Leutwyler, R. A. Bachorz, W. Klopper, *J. Phys. Chem. B* **2009**, *113*, 2937. c) I. Dauster, C. A. Rice, P. Zielke, M. Suhm, *Phys. Chem. Chem. Phys*. **2008**, *10*, 2827.

[15] M. Nishio, M. Hirota, Y. Umezawa, *The CH/π Interaction. Evidence, Nature and Consequences*, Wiley-VCH, New York, **1998**.

[16] a) S. Grimme, *Angew. Chem. Int. Ed*. **2008**, 47, 3430. b) P. Hobza, *Phys. Chem. Chem. Phys*. **2008**, *10*, 2581. c) E. A. Meyer, R. K. Castellano, F. Diederich, *Angew. Chem. Int. Ed*. **2003**, *42*, 1211. d) T. Goly, U. Spoerel, W. Stahl, Chem. Phys. 2002, 283, 289.

[17] A. L. Llamas-Saiz, C. Foces-Foces, O. Mo, M. Yáñez, J. Elguero, *Acta Crys*. **1992**, *B48*, 700

[18] a) G. A. Jeffrey, H. Maluszynska, *Acta Cryst*. **1990**, *B46*, 546. b) B. Piraud, G. Baudoux, F. Durant, *Acta Cryst*. **1995**, *B51*, 103.

[19] a) P. Hobza, K. Müller-Dethlefs, *Non-Covalent Interactions*, RSC Pub., Cambridge, **2010**. b) K. E. Riley, P. Hobza, *WIREs: Comput. Mol. Sci.* **2011**, *1*, 3.

[20] B. Temelso, K. L. Klein, J. W. Mabey, C. Pérez, B. H. Pate, Z. Kisiel, G. C. Shields, *J. Chem. Theory Comput.* 201814, 1141.

[21] L. Goerigk, S. Grimme, *J. Chem. Theory Comput.* **2011**, *7*, 291.

[22] L. Gráfová, M. Pitoňák, J. Řezáč, P. Hobza, *J. Chem. Theory Comput.* **2010**, *6*, 2365.

[23] S. T. Schneebeli, A. D. Bochevarov, R. A. Friesner, *J. Chem. Theory Comput.* **2011**, *7*, 658.

[24] T. Risthaus, S. Grimme, *J. Chem. Theor. Comp.* **2013**, *9*, 1580.

[25] Y. Zhao, D.G. Truhlar, *Theor. Chem. Account.* **2006**, *120*, 215–241.

[26] S. Grimme, J. Antony, S. Ehrlich, H. Krieg, *J. Chem. Phys.* **2010**, *132*, 154104.

[27] D. Schemmel, M. Schütz, *J. Chem. Phys.* **2010**, *132*, 174303.

[28] a) I. León, P. F. Arnaíz, I. Usabiaga, J. A. Fernández, *Phys. Chem. Chem. Phys.* **2016**, *18*, 27336. b) I. León, I. Usabiaga, P. F. Arnaiz, A. Lesarri, J. A. Fernández*, Chem. Eur. J.* **2018**, *24*, 10291.

[29] D. Bernhard, F. Dietrich, M. Fatima, C. Pérez, H. C. Gottschalk, A. Wuttke, R. A. Mata, M. A. Suhm, M. Schnell, M. Gerhards, *Beilstein J. Org. Chem.* **2018**, *14*, 1642.

[30] H. C. Gottschalk, J. Altnöder, M. Heger, M. A. Suhm, *Angew. Chem. Int. Ed.* **2016**, *55*, 1921.

[31] a) S. T. Shipman and B. H. Pate, in *Handbook of High Resolution Spectroscopy*, ed. M. Quack and F. Merkt, Wiley, New York, 2011, pp. 801–828. b) J.-U. Grabow, in *Handbook of High Resolution Spectroscopy*, ed. M. Quack and F. Merkt, Wiley, New York, 2011, pp. 723–800.

[32] E. Ye, K. Chandrasekaran, R. P.A. Bettens, *J. Mol. Spectrosc.* **2005**, *229*, 54.

[33] U. Spoerel, W. Stahl, *J. Mol. Spectrosc.* **1998**, *190*, 278.

[34] D. Consalvo, V. Storm, H. Dreizler, *Chem. Phys.* **1998**, *228*, 301.

[35] K.-I. Sugawara, J. Miyawaki, T. Nakanaga, H. Takeo, G. Lembach, S. Djafari, H.-D. Barth, B. Brutschy, *J. Phys. Chem.* **1996**, *100*, 17145.

[36] E. R. Johnson, S. Keinan, P. Mori-Sánchez, J. Contreras-García, A. J. Cohen, W. Yang, *J. Am. Chem. Soc.* **2010**, *132*, 6498.

[37] J. Contreras-García, E. R. Johnson, S. Keinan, R. Chaudret, J.-P. Piquemal, D. N. Beratan, W. Yang, *J. Chem. Theory Comput.* **2011**, *7*, 625.

[38] F. N. Keutsch, J. D. Cruzan, R. J. Saykally, *Chem. Rev.* **2003**, *103*, 2533.

[39] A. L. Llamas-Saiz, C. Foces-Foces, *J. Mol. Struct.* **1990**, 238, 367.

[40] A. L. Llamas-Saiz, C. Foces-Foces, O. Mo, M. Yáñez, *Acta Cryst.* **1992**, B48, 700.

[41] S. Grimme, M. Steinmetz, *Phys. Chem. Chem. Phys.* **2016**, *18*, 27336.

[42] I. Usabiaga, J. González, I. León, P. F. Arnáiz, E. J. Cocinero, J. A. Fernández, *J. Phys. Chem. Lett.*, **2017**, *8*, 1147.

Entry for the Table of Contents
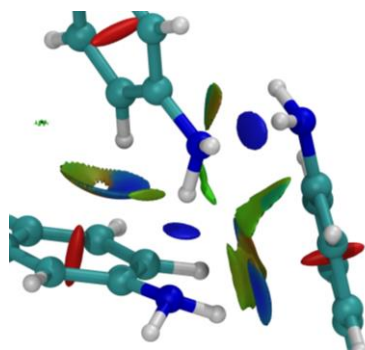
Weaker hydrogen bonds favour competing isomerism in neutral molecular clusters, as observed in five isomers of the aniline trimer and the hydrated aniline dimer

Figure 1. The microwave spectrum of aniline (2-8 GHz) and an enlarged 30 MHz window comparing typical rotational transitions for An_3 and An_2-W (negative trace, water added). Transitions of the symmetric trimer and additional spectra are illustrated in Figures S1-S3 (SI).
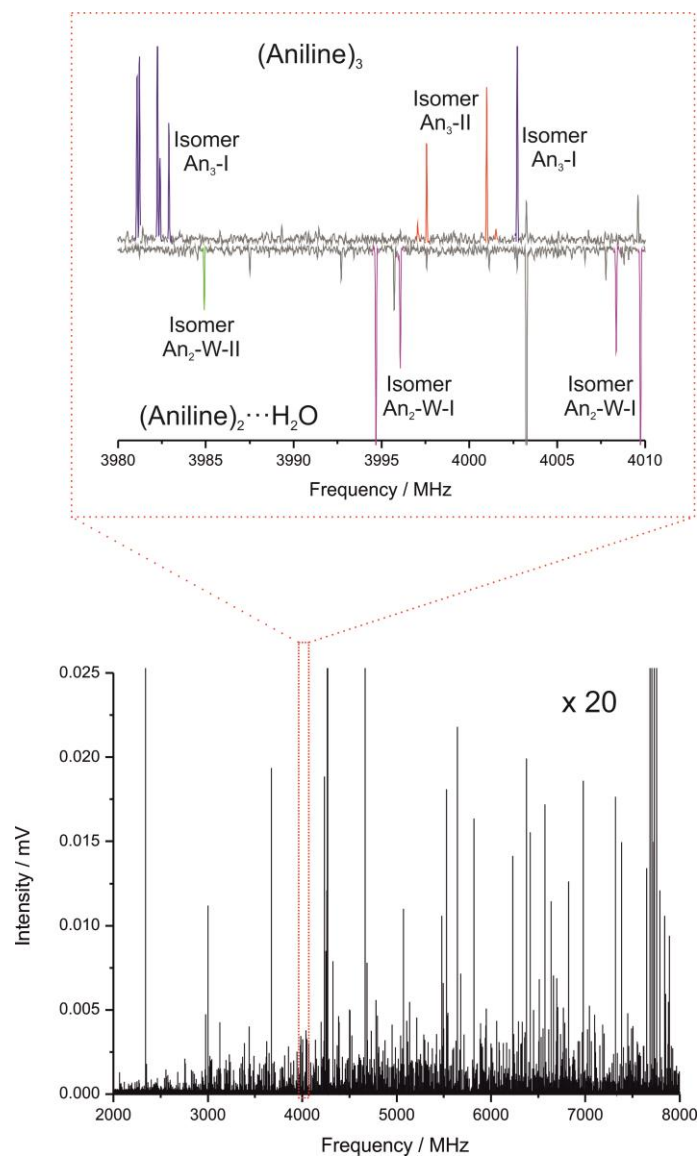
Figure 2. The three observed isomers of An$_3$, with intermolecular interactions mapped by NCI plots (hydrogen bonds in blue, weak stabilizing interactions in green, destabilizing interactions in red). All isomers show dominant N-H$\cdots$N hydrogen bonds, with assistance of N-H$\cdots\pi$ and C-H$\cdots\pi$ weaker interactions.
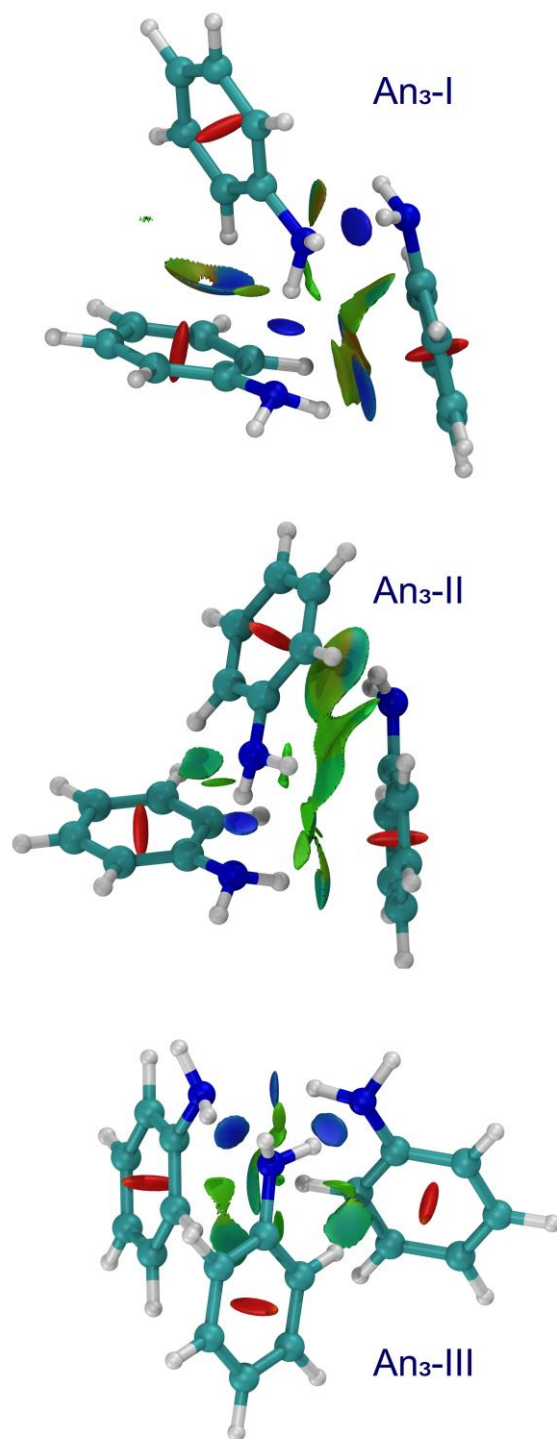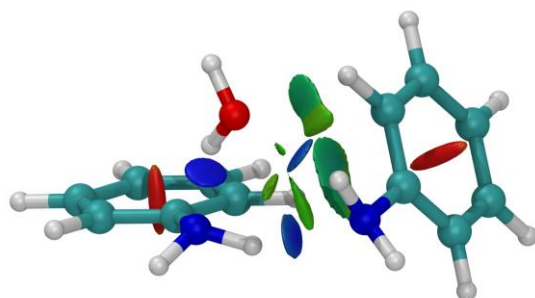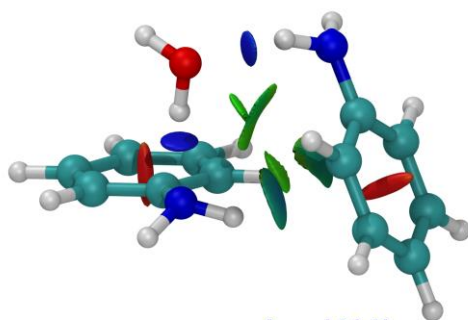
Figure 3. The two isomers of An$_2$-W and NCI plots. Both trimers are primary stabilized by water, acting as hydrogen bond bridge between the two aniline molecules.

An$_2$-W-I

An$_2$-W-II

Table 1: Experimental rotational parameters of the ^{15}N-aniline trimer and the monohydrated dimer.

	An$_3$-I[b]	An$_3$-II	An$_3$-III	An$_2$-W-I	An$_2$-W-II
A /MHz[a]	374.521823(81)	312.64137(10)		733.67814(50)	791.873(24)
B /MHz	225.824064(55)	292.926220(76)	264.85980(40)	374.98271(73)	351.33331(50)
C /MHz	178.768887(64)	209.026782(80)		289.06386(71)	309.72735(46)
D_J /kHz	0.02574(16)	0.01718(31)	0.4262(12)	0.1647(69)	0.4743(14)
D_{JK} /kHz	-0.03846(66)	0.0287(17)			-1.3054(90)
D_K /kHz	0.17271(51)	-0.0064(19)			-20.7(25)
d_1 /Hz	-4.516(96)	-3.41(14)			-0.1547(10)
d_2 /Hz	-0.337(42)	-1.010(99)			
σ /kHz	3.6	4.1	7.5	12.7	7.5
N	260	213	8	51	71

[a]Rotational (A, B, C) and Watson's S-reduced centrifugal distortion constants (D_J, D_{JK}, D_K, d_1, d_2), standard deviation of the fit (σ) and number of transitions (N). [b]Standard error in units of the last digit.